The 2019 Resumption of Activity on Avachinsky Volcano

P. P. Firstov[a], *, **A. A. Shakirova**[a], **, **A. P. Maksimov**[b], and **E. V. Chernykh**[b]

[a] *National Seismological Centre, Geophysical Survey, Russian Academy of Sciences,*
Petropavlovsk-Kamchatsky, 683006 Russia

[b] *Institute of Volcanology and Seismology, Far East Branch, Russian Academy of Sciences,*
Petropavlovsk-Kamchatsky, 683006 Russia

*e-mail: firstov@emsd.ru

**e-mail: shaki@emsd.ru

Abstract—The waveforms and spectral content of the earthquakes that were recorded during the period of higher activity on Avachinsky Volcano in 2019 were studied to identify three commonly accepted types of volcanic earthquake (VE), viz., volcano-tectonic, hybrid, and long-period events, as well as a fourth type, a "special" VE type having certain special features in its waveforms. We have identified 15 plane-oriented clusters and determined characteristics of the seismogenic planes. An analysis of the seismic events that were recorded in the fall of 2019 on the Molodoi Konus of Avachinsky Volcano suggests that the resumption of activity was related to the magma bodies due to the 1991 eruption which exist in the cone body and to their interaction with atmospheric precipitation. The most likely cause of light flashes above the crater observed on December 8 seems to have been interaction between hydrogen-charged volcanic gas and air oxygen.

INTRODUCTION

Eruptions of Avachinsky Volcano[1], which is situated near the Krai center, Petropavlovsk-Kamchatsky (23 km) and the Elizovo international airport (30 km), pose potential hazard for this agglomeration with over 200000 residents (Fig. 1a). For this reason the 2019 resumption of activity excited special interest of the scientific community (Malik and Nekrasova, 2020; Muraviev, 2020; Shakirova et al., 2020).

The volcano's morphology identifies it as belonging to the Somma-Vesuvius type: the Holocene Molodoi Konus volcano is situated in the crater of the Late Pleistocene Paleo-Avacha volcano, which bears relationship to all recent activity. Fifteen eruptions are known to have occurred since 1737 until today with considerable differences in character and intensity (Melekestsev et al., 1994, 2002).

The largest explosive eruption of the subplinian type in 1945 resulted in a crater ~250 m across and a depth of ~170 m. The next eruption of January 1991 was largely effusive. The eruption produced a thick lava plug in the crater of volume 8.3×10^6 m³, and a lava flow was discharged onto the volcano's slopes ($V = 4.4 \times 10^6$ m³) (Melekestsev et al., 1994; Ivanov et al., 1995). The next eruption of October 5, 2001

occurred as a weak gas explosion ~1000 m high above the crater, emitting some ash and fragments of the 1991 eruption. The event resulted in a ravine-like fissure that traverses the lava plug NW–SE at an azimuth of 325° (Melekestsev et al., 2002).

A thermal survey was carried out on November 6, 2001; it showed thermal anomalies at the center of the fissure and along its edges, with the projection of the fissure center being identical with the thermal anomaly in the bottom part of the crater where lava began to flow in 1991 (Dubrovskaya et al., 2019). Inspection of the fissure images revealed outlines of funnels that seem to have been produced by the explosion (see Fig. 1b, inset). It should be noted that in both cases, the eruptions were preceded by volcanic earthquakes (VE) with energy class $K < 6.6$ ($K = \log E$, J) that largely occurred in the volcanic edifice (Senyukov et al., 2006). However, the comparatively low seismic activity in the former of these cases and an absence of any experience in eruption prediction for this volcano in the latter case prevented short-term forecasts for the two eruptions.

Avachinsky Volcano typically shows persistent fumarolic activity with a whole network of distinct fumaroles aligned along the periphery of the crater and at the ends of the fissure. The fumaroles have temperatures varying within wide limits, with the most

---

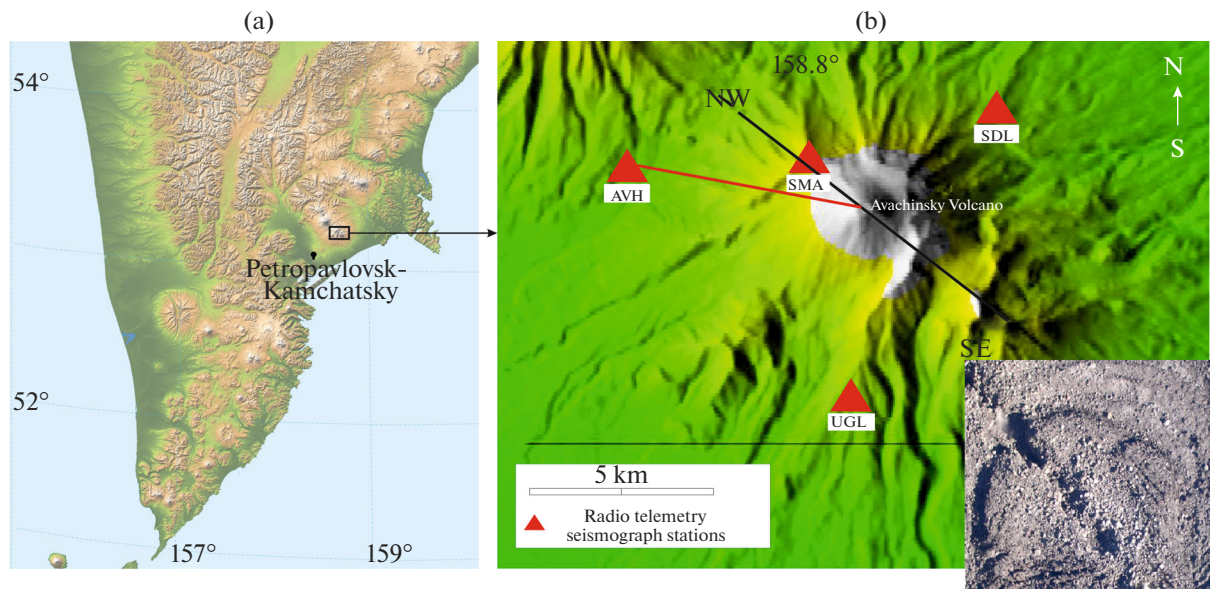[1] http://geoportal.kscnet.ru/volcanoes/volc?name=Avachinsky.

Fig. 1. The location of Avachinsky Volcano (a) and the RTSSs in its environs (b).

Inset: the fissure that formed in the plug after the 2001 eruption. Red line indicates the direction of view for the video camera at the RTSS AVH. RTSS names: AVH Avacha, SMA Somma, SDL Sedlovina, UDL Uglovaya. Photographed by I.K. Dubrovskaya on June 28, 2005.

vigorous among these reaching temperatures in excess of 600−800°C (Malik et al., 2017).

The period of October to December 2019 saw an increase in the Avachinsky seismicity. Luminescence was recorded in the western part of the crater since October 27 by the infrared camera operated by the National Seismological Centre, Geophysical Survey, Russian Academy of Sciences installed at the Avacha radio telemetry seismic station (AVH RTSS) at a distance of 6 km from the volcano's crater (see Fig. 1b) (http://www.emsd.ru/~ssl/monitoring/main.htm). Visual observation recorded increased fumarolic activity and a high concentration of gas in the crater during that period.

This study provides a detailed account of the Avachinsky activity in late 2019 with emphasis on seismicity, and considers a plausible explanation of possible mechanisms responsible for the activity.

BRIEF INFORMATION ON VOLCANIC EARTHQUAKES

Since the 1950s, "volcanic seismology" has been evolving as a scientific discipline, it faced the problem of classification with regard to earthquakes associated with volcanic activity, i.e., those which preceded and accompanied eruptions. One of the earlier attempts at classifying the VEs on the basis of their records and their relationship to volcanic activity was undertaken by G.S. Gorshkov (1954a). Because earthquakes were recorded at that time in analog form and low drum

speeds, his classification was rather simplistic. His next study (Gorshkov, 1954b) dealt with terminology, providing the first definition of "volcano-tectonic" earthquakes as ones with the waveforms of tectonic ones, but which occurred in areas of active volcanoes.

The well-known classification scheme due to the Japanese researcher Minakami (1961) was based on the relationship between VEs and the activity of volcanoes and the locations of their chambers. Later on, P.I. Tokarev (1966) identified five VE types based on the eruptions of Kamchatkan volcanoes, and these types are consistent with the Minakami classification. This classification scheme is in use at present among Russian volcanologists.

Later, when digital recording and computer location of earthquakes began to be used in seismology, it proved possible to do a more detailed study of VE waveforms and to obtain greater accuracy for the location of low magnitude VEs. This gave the impetus to the development of a new classification for VEs, see (McNutt, 1996; Power et al., 1994; Gordeev and Senyukov, 1998; Zobin, 2017). Three main types of VEs are distinguished: volcano-tectonic, hybrid, and long-period events; these types will be discussed using the earthquakes recorded during the renewed activity of Avachinsky Volcano in 2019.

Apart from these VE types, which are observed on all volcanoes worldwide, there have been occasional instances of another type, "tornillo" ("screw", TE), which is characterized by monochrome frequency spectrum and longer coda-wave durations (Cannata

et al., 2012; Gomez, 1999). As an example, the seismicity increases on Vulcano[2] (Aeolian Islands, Italy) that were similar to that on Avachinsky, were accompanied by concurrent VEs which were explained by interaction between the aqueous fluid and a magma body (Milluzzo et al., 2010). As well, VEs were also observed on Galeras Volcano, Central Andes before and after eruptions (Gomez, 1999).

TEs and VEs with special waveforms were recorded during the seismicity increase on Iwo Jima Volcano, Japan in September 1997. This VE type consisted in a short record of low amplitude oscillations (*emergent phase*) that preceded the main shock. It is also hypothesized that earthquakes such as these can be excited by gas bubbles with subsequent destruction of highly viscous rhyolite magma (Uchida and Sakai, 2002).

OBSERVATION PROCEDURES AND DATA PROCESSING

The activity of Avachinsky Volcano is continuously monitored visually using a digital IP-camera installed at the RTSS AVH situated at a distance of 6 km from the crater (see Fig. 1b). The video camera can conduct surveys in visible and infrared ranges, which can monitor the dynamics of fumarolic activity (intensity and temperature) above the volcano's crater. The camera has recorded rather interesting events during the resumption of activity in late 2019. The data concerning the monitoring of volcano activity were taken from the site of the National Seismological Centre, Geophysical Survey, Russian Academy of Sciences (NSC GS RAS) (http://www.emsd.ru/~ssl/monitoring/main.htm)

The seismicity recorded in the area of Avachinsky Volcano is monitored by a network of four RTSSs situated at distances of 2.4 km to 6 km from the volcano's crater (see Fig. 1b). This network can be used to locate weak VEs in the volcanic edifice, energy class $K_S \geq 1.5$ ($K_S = \log E$, J).

The three-component instrumentation of short-period channels (SH) based on the SM3 seismometer ($T_S = 1.2$ s) can record ground motion velocity in the frequency band 0.8–20 Hz. The RTSSs have a highly sensitive channel to record weak earthquakes, which can record the vertical component (EHZ) with a resonant characteristic in the frequency band 8–12 Hz at level 0.7. Earthquake records are tied to Coordinated Universal Time, UTC, which is also used in the present paper.

Earthquake location was based on a local 1D velocity model that allows for location of hypocenters above sea level (Senyukov, 2006). The location uncertainty for the Avachinsky area is estimated as approximately one kilometer both in map view and over depth

(Nuzhdina et al., 2019). The earthquake parameters processed in real time were analyzed in the study referred to and have been published in the service web data base of the NSC GS RAS (http://www.emsd.ru/ts/). Earthquake location and the calculation of earthquake parameters were carried out using the DIMAS interactive program (Droznin and Droznina, 2010, 2011). The hypocenter depths above sea level have the plus sign and those below sea level are marked with the minus sign.

Kiryukhin et al. (2016, 2017) and Kiryukhin (2017) have developed a procedure for identifying plane-oriented clusters in VEs based on the following criteria: (1) a time limitation on events, less than 24 hours; (2) the scatter of earthquake hypocenters in the horizontal plane, ≤6 km; (3) their distance from the seismogenic plane, ≤200 m; (4) the number of earthquakes in a cluster, ≥6. The seismicity increase on Avachinsky Volcano in 2019 was found to contain plane-oriented clusters in the interactive Frac-Digger program (no. 2016616880)[3].

SEISMIC EVENTS RECORDED IN THE AVACHINSKY AREA IN OCTOBER–DECEMBER 2019

VEs of different types were recorded in the area of the Avachinsky edifice since the end of October 2019.

The identification of VE types during the 2019 seismicity increase on Avachinsky was based on earthquake waveforms and the spectral content as recorded at the RTSS SMA station, which is the nearest to the volcano. The three commonly accepted types have been identified in addition to the fourth, "special" VE type.

The volcano-tectonic earthquakes (VTE) due to brittle fracture in the geological material had distinct arrivals of *P* and *S* waves, and $t_{s-p} = 0.8$ s (Fig. 2a). The VTE spectrograms were found to contain intensive amplitude densities with frequencies in the range $f = 12-15$ Hz (Fig. 3a).

Hybrid earthquakes (HE) are characterized by clear onsets with $t_{s-p} = 0.9$ s followed by records of obvious coda waves at lower frequencies (see Fig. 2b). The HE spectrogram involves two spots of density $f_1 = 6$ Hz in the initial segment of the record and with $f_2 \approx 2$ Hz for coda waves (see Fig. 3b). The mechanism responsible for HE generation is commonly related to brittle filling of the geological medium resulting in the formation of a fissure and subsequent filling of it with magma or fluids (Gordeev and Senyukov, 1998).

Long period earthquakes (LPE). These typically involve emergent onsets of *P* and *S* and a relatively lower frequency compared with the preceding types

---

[2] The names of volcanoes are after I.I. Gushchenko's catalog (1979).

[3] *Kiryukhin, P.A. and Kiryukhin, A.V.,* Frac-Digger. Certificate of State Registration for computer program no. 2016612168 as of June 21.
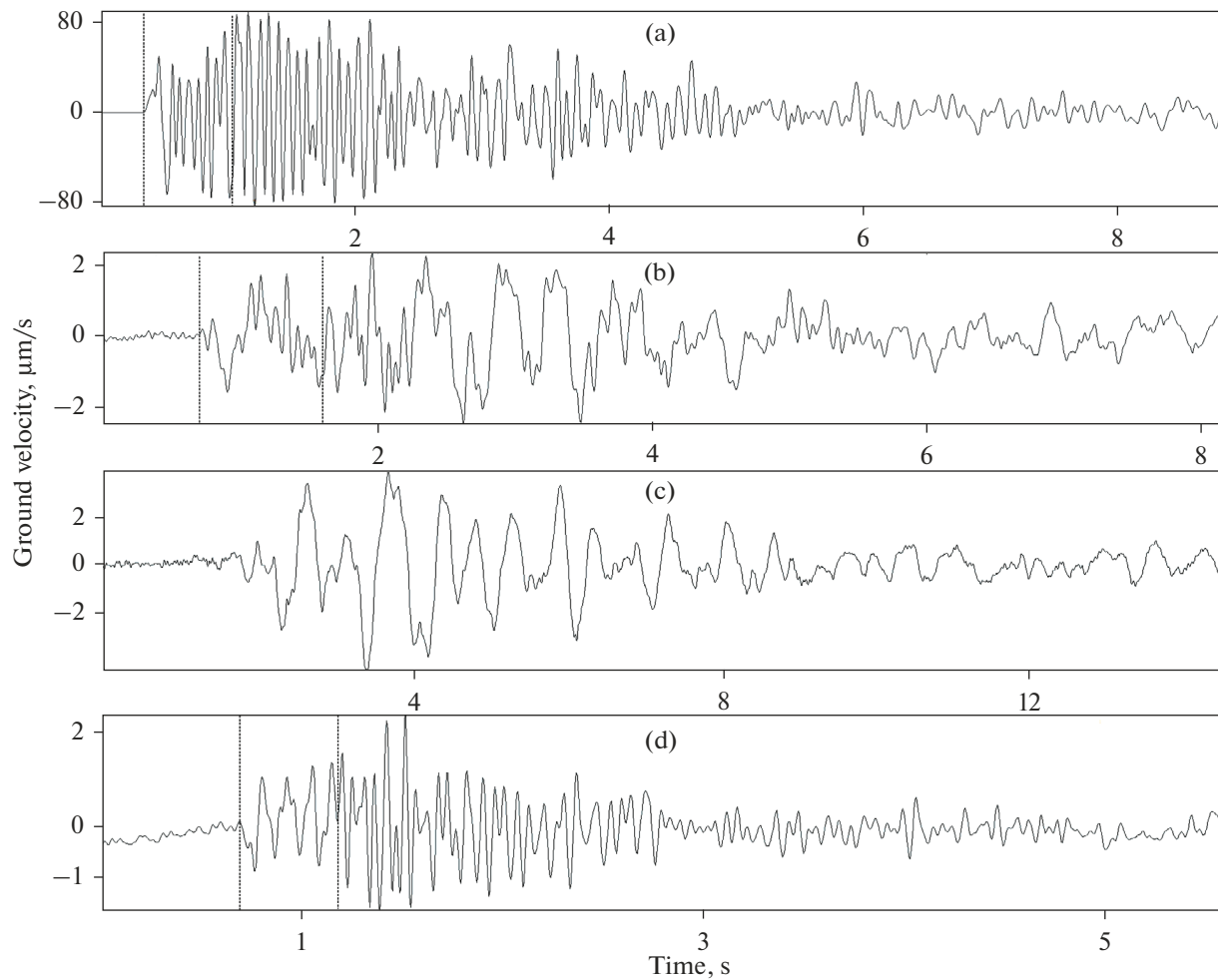
Fig. 2. The waveforms of the earthquakes recorded on the vertical component at RTSS SMA (SHZ) during the resumed activity of Avachinsky Volcano in October–December 2019.

(a) VT earthquake of December 9, 2019 at 14:54 with Ks = 6.6, H = –1.42 km; (b) HE of December 10, 2012 at 23:03 with Ks = 3.5, H = 1.8 km; (c) LPE of November 18, 2019 at 09:09 with Ks = 2.7, H = 1.8 km; (d) "special" earthquake of November 5, 2019 at 11:46 with Ks = 3.6, H = 1.8 km.

(see Fig. 2c). The spectrogram contains a spot of spectral density at $f \approx 1.5-2$ Hz during 5 s (see Fig. 3c). It is thought that the LPE mechanism involves fracture of a geological material of low density or a fracture filled with magma/fluid. LPEs are frequently observed before eruptions, when the pressure in the conduit of a volcano or in fissures increases due to the arrival of a fresh magma portion.

Special earthquakes (SE). Nine earthquakes of K_s = 1.9–4.2 were recorded during the seismicity increase. The waveforms of these earthquakes differed from those on the commonly accepted classification of VEs. The initial segments in the records of such earthquakes were dominated by lower frequencies compared with the coda waves (see Fig. 2d). We have called them "special" earthquakes; these had relatively short records involving sharp onsets of P and t_{s-p} = 0.5 s at the RTSS SMA. Their waveforms and frequency spec-

tra were similar to the *main phase* of *special-type* earthquakes which were recorded during the low intensity activity on Iwo Jima Volcano, Japan (Uchida and Sakai, 2002). The SE spectrogram contains five linear spots of spectral density with frequencies f_1 = 8 Hz, f_2 = 10 Hz, f_3 = 12 Hz, f_4 = 14 Hz, and f_5 = 21 Hz (see Fig. 3d), with the frequency f_5 = 21 Hz arriving after the S onset.

Overall, the spectrograms clearly show differences in spectral content for the VE types as recorded during the seismicity increase on Avachinsky in late 2019 (see Fig. 3).

Consider some features of the SE. The first arrival of P in SEs was generally positive (7 of 9). Such earthquakes may have been due to "explosive" processes occurring in the volcanic cone. This hypothesis is corroborated by particle paths in first arrivals in the EW-Z and NS-Z planes, which are close to the direction
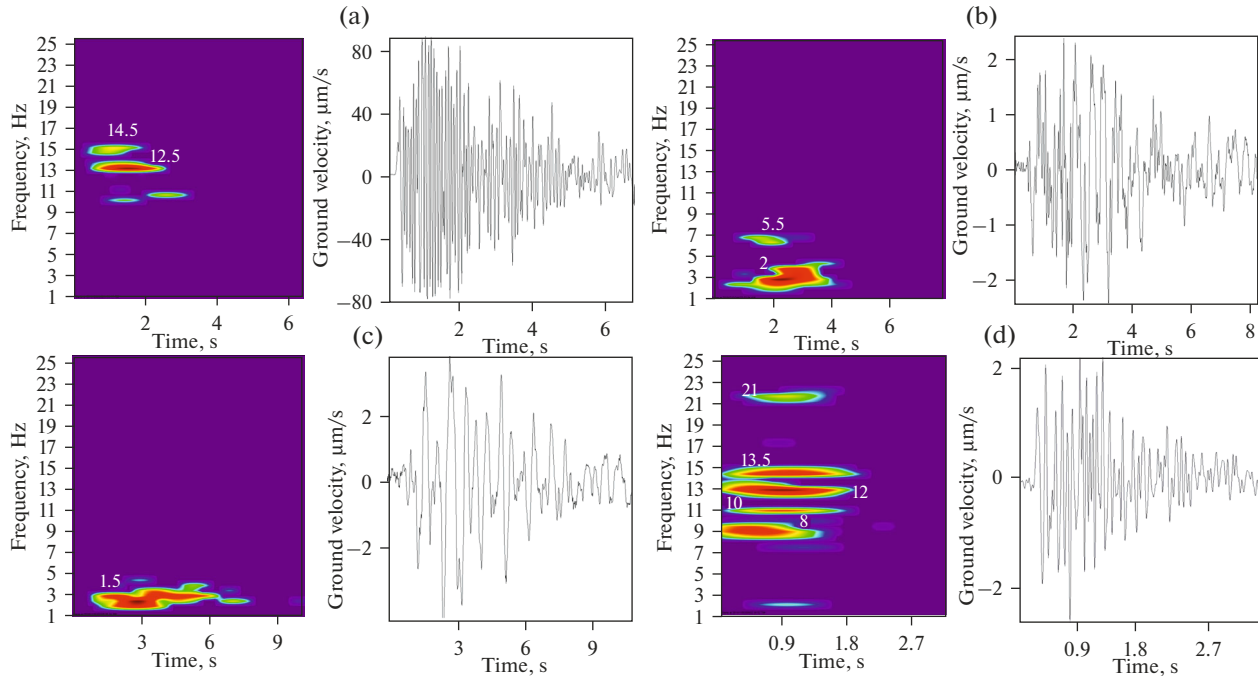
Fig. 3. The spectrograms of four VE types recorded on the vertical component (SHZ) of RTSS SMA during the resumed activity of Avachinsky Volcano in October−December 2019. (a) VTE of December 9, 2019 at 14:54 with Ks = 6.6, H = −1.42 km; (b) HE of December 10, 2012 at 23:03 with Ks = 3.5, H = 1.8 km; (c) LPE of November 18, 2019 at 09:09 with Ks = 2.7, H = 1.8 km; (d) "special" earthquake of November 5, 2019 at 11:46 with Ks = 3.6, H = 1.8 km.

toward the source (Fig. 4) as observed in the near zone during excavation explosions or near an interface with a big contrast in material properties (Romashev, 1980).

The seismicity increase terminated in weak high frequency spasmatic tremor that began to be recorded at the RTSS SMA at ~04:00 on December 25 and ceased at 11:00 on December 26 (Figs. 5a, 5b). The amplitude spectrum clearly shows three spectral peaks, a "low frequency" one at f_1 = 5 Hz and two distinct "high frequency" peaks at f_2 = 19 Hz and f_3 = 23.5 Hz (see Fig. 5c). This spectral structure is similar to that of the SEs where close-spaced frequencies are identified as well. In addition, this period saw an increase in fumarolic activity. Volcanic tremor (VD) might have been caused by vigorous movement of fluids along a permeable zone due to the seismicity increase.

LUMINESCENCE OBSERVED ON THE CRATER OF THE VOLCANO

A video recorder was used to capture weak luminescence in the middle of the crater outline from out the RTSS AVH in the night of October 27, 2019. The luminescence was seen as a spot that was periodically recorded until the end of December. A unique phenomenon was observed from 11:23 to 12:15 on December 8, when five flashes of varying intensity were recorded at the location of the luminescence (Fig. 6). Comparison of the aspects of light spots averaged in an interval of one minute suggests that these spots were generated by explosive processes at different depths. The brightest flash took place at 12:15 (see Fig. 6a). The aspect of the light spot suggests that it may have been generated by an explosive process due to interaction between explosion-prone volcanic gases and air oxygen. The semi-spherical shape and the scatter of explosion products show that the explosion probably occurred below the crater surface.

Unfortunately, the air wave was not recorded by acoustic stations in Kamchatka because of the great distances between these and the volcano. However, weak seismic signals were recorded in the high frequency channel of the RTSS SMA in a time vicinity of the two largest flashes at 12:11 and 12:15 (Figs. 7b, 7c). In the first of these cases two seismic signals were recorded spaced at an interval of 7 s. The character of their waveforms reminds one of SEs. The second flash was accompanied by a relatively high frequency narrow-band signal that is very much like ground motion due to the impact of a shock wave in air. The duration of the seismic signal (~15 s) and the long luminescence due to the flash may indicate a multiact character of the process.
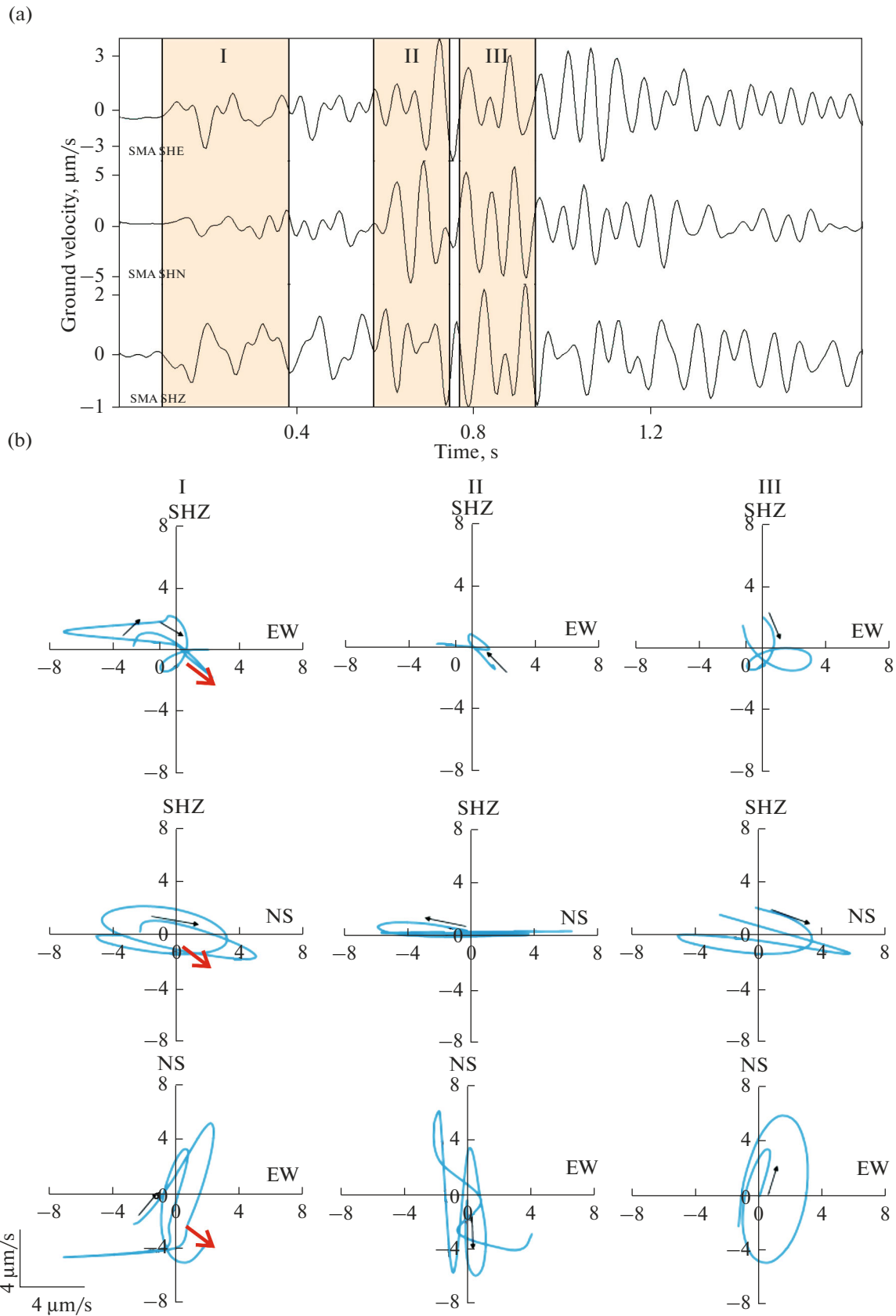
(a)

(b)

Fig. 4. A sample SE recorded on November 5, 2019 at RTSS SMA (a); particle path in different wave groups (b). Red arrows indicate the direction toward the crater center, black arrows show the direction of ground motion. The time origin is at 11:46:35.
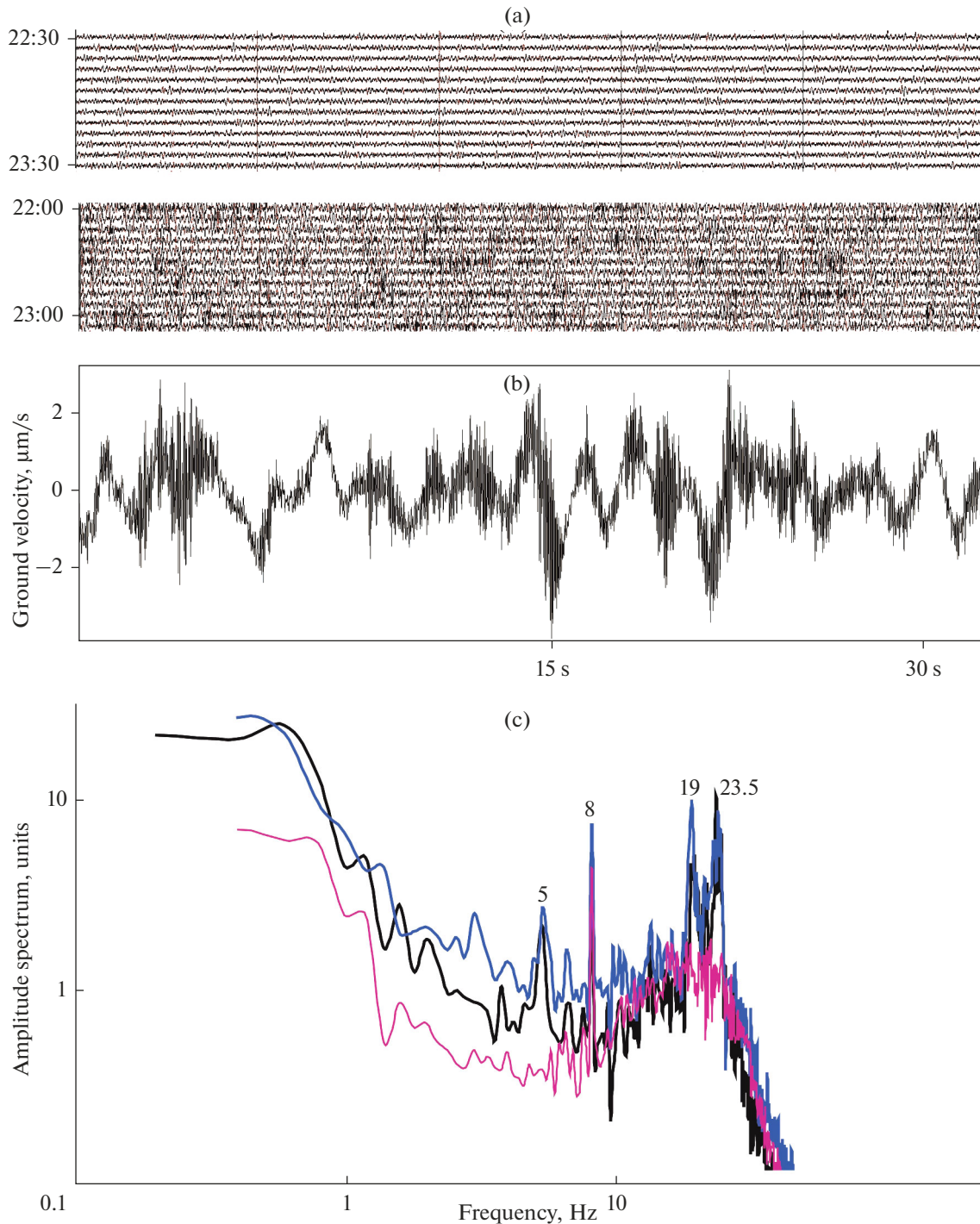
Fig. 5. Fragments of one-hour records on the vertical component (SHZ) at RTSS SMA made on December 24, 2019 in the absence of VT and on December 25 with VT (a); a fragment of a VT record lasting 30 s on the vertical component (SHZ) at RTSS SMA (b); amplitude spectra for two segments of VT and for background (c). The time origin is 21:33:30 (in Fig. 5b).

THE DYNAMICS OF SEISMICITY ON AVACHINSKY VOLCANO IN LATE 2019

The seismicity on the volcano in late 2019 consisted of six swarm sequences of volcanic earthquakes which are clearly seen in the cumulative curve of the number of earthquakes (see Fig. 7d). The bulk of hypocenters were above sea level ($0 < h < 2$ km) and tended to cluster near two horizons, ~0.5 and ~1.8 km b. s. l., while the epicenters were concentrated in the north-northeastern sector of the volcanic cone (see Figs. 7a, 7b). Th energy class values were in the range
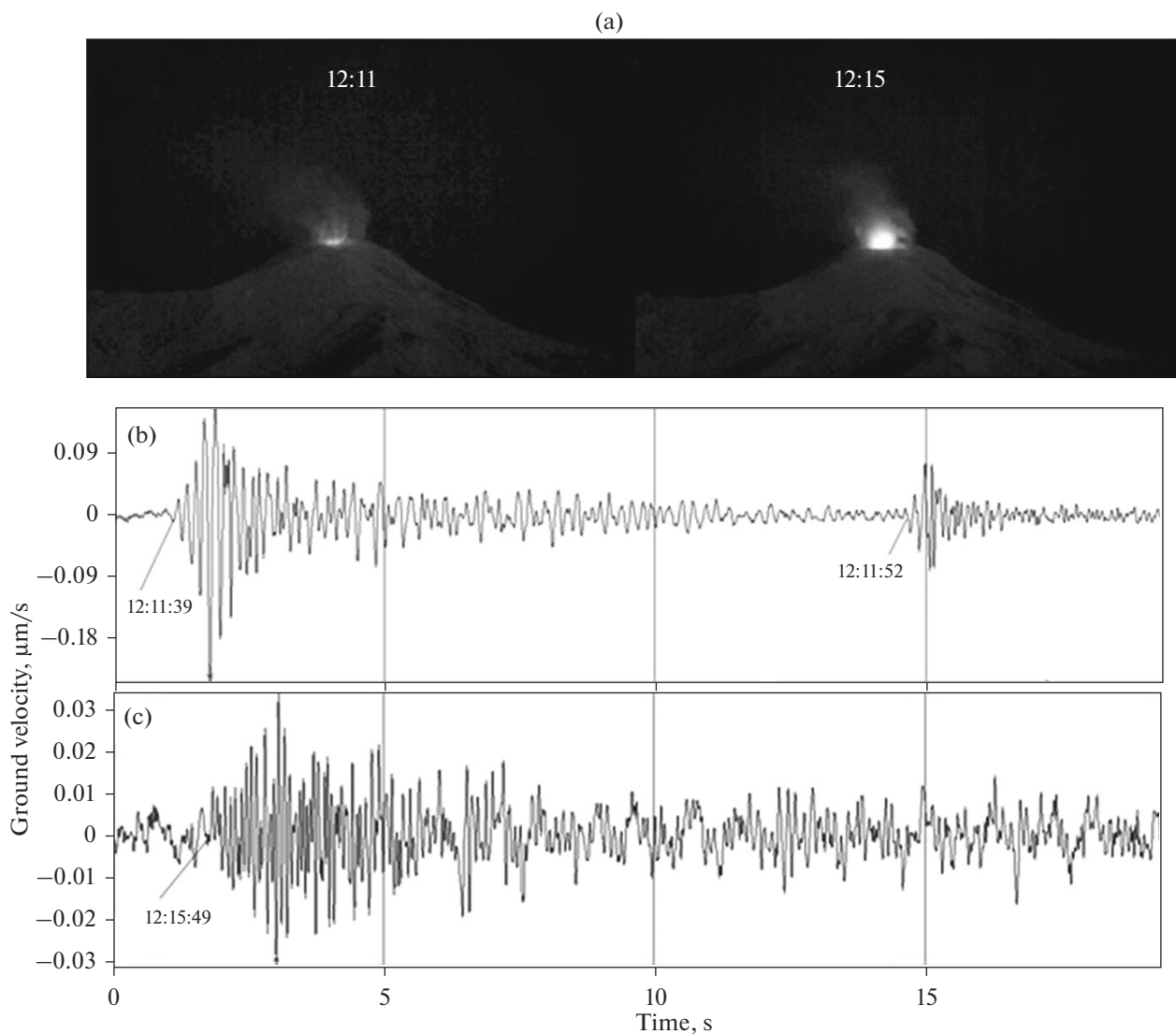
Fig. 6. The brightest flashes recorded by a camera at RTSS AVH at 12:11 and 12:15 (a); fragments of seismic records on the HF channel at RTSS SMA corresponding to the time intervals of flashes at 12:11 (b) and at 12:15 (c) on December 8, 2019. The time origin is 12:11:37 for (b) and 12:15:47 for (c).

$1.4 < K_S < 6.6$. The greatest energy was released by the 5th swarm which contained the largest earthquakes with $K_S = 6.6$ (see Fig. 7c).

Fifteen plane-oriented clusters were identified by the procedure outlined above during the period of seismic activity on Avachinsky Volcano, October to December 2019; the cluster centers were in the range of depths between 302 and 1842 m (Table 1, Fig. 8). The figures just quoted to within one meter resulted from computer identification of cluster parameters. We are quite aware of the fact that the location uncertainty was large enough to prevent us from giving this high accuracy, but these constructions are quite justified in the process of looking for general patterns in earthquake clustering exhibited by swarm sequences.

Two clusters were identified in swarm sequences during the start of the seismicity increase and three clusters at the end. The clusters were mostly subvertical dipping at angles of 59° to 84°, but clusters 1, 8, and 12 were nearly horizontal and their centers were at a height of ~1800 m (Shakirova et al., 2020). We examined the percentage of VE types in the clusters (see inset in Fig. 8a). The overwhelming majority of the earthquakes were of two types, VTE and LPE. VTEs were prevalent during the initial period of the seismicity increase: clusters 5 and 7 were wholly of VTEs, while the percentage of such events was much lower in the last four clusters. The picture is reversed for LPEs. Hybrid earthquakes were only recorded in cluster 12, while SEs occurred only during the earlier half of the seismicity increase (see inset in Fig. 8a).
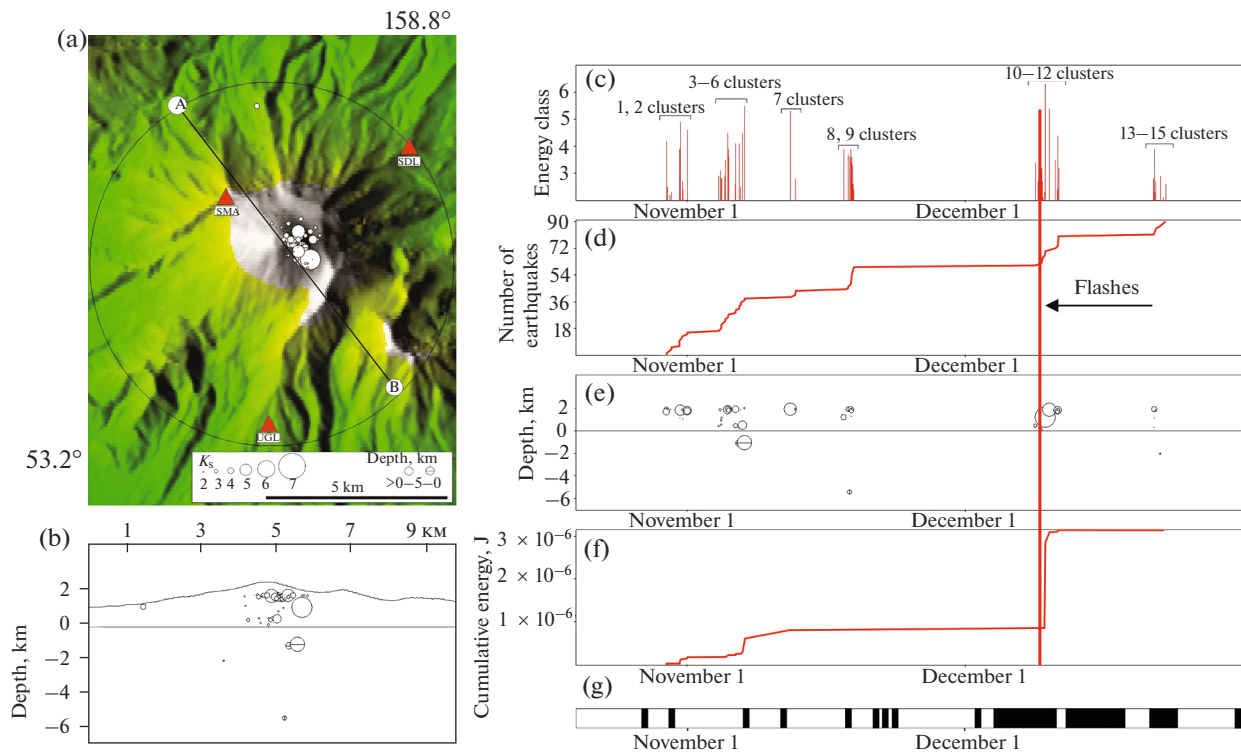
Fig. 7. A map showing the epicenters of earthquakes that occurred in the Avachinsky edifice in October−December 2019 (a); hypocenters projected onto the vertical plane along the A−B line (b); time-dependent distribution of energy class (K) (c); cumulative curve of the number of earthquakes (d); hypocenter depths (e); cumulative curve of earthquake energy (f); luminescence in the middle of the crater (g) (http://www.emsd.ru/~ssl/monitoring/main.htm). The vertical line marks the period of observed explosions in air. RTSS names: SMA Somma, SDL Sedlovina, UGL Uglovaya.

DISCUSSION OF RESULTS

These results from the analysis of seismic events occurring in October−December 2019 suggest certain inferences concerning the character of the seismicity increase on Avachinsky Volcano and a likely scheme for the responsible mechanism.

Nearly all earthquakes concentrated in the Molodoi Konus edifice were weak, ($1.4 < K_S < 6.6$). The centers of the clusters were at heights of ~300−1850 m. At the same time, geophysical evidence tells us that a peripheral magma chamber is at a depth of 0 to 2 km according to Moroz and Gontovaya (2003) and at depths of 2 km below the ground surface according to Bushenkova et al. (2019). This points to an absence of a relationship between the seismicity increase and the processes occurring in the volcanic chamber.

The seismicity increase occurred from late October to December 2019. Similar increases in seismic activity occurred in February−April 1996, late August to October 2001, and October−November 2005 (Senyukov et al., 2006). Practically all seismicity increases concerned the central part of the cone edifice between sea level and the crater. The 2001 increase also involved a weak explosion discharging a small amount of ash and smaller blocks, when the plug in the crater failed and a fissure was formed in it. The 2005 activity

was accompanied by a weak thermal anomaly and a few hybrid earthquakes, as was also the case for 2019 (Senyukov et al., 2006).

These seismicity increases clearly show a definite relationship to the seasons of the year, with all of these occurring during transitional periods, fall−winter or winter−spring. This may indicate a relationship between the seismicity increases and sharp increases in the concentration of water in the volcanic cone due to higher precipitation in the fall season and the breakup of snow and ice on the cone in the spring. The Molodoi Konus is mostly composed of unconsolidated volcanic deposits with some interbeds of lava flows and sills, i.e., is comparatively permeable to meteoric water. Atmospheric water as rain or thaw water penetrates the cone much less in summer when the cone is free of snow and ice, and likewise in winter, when the cone is shielded by a layer of ice and snow.

The presence of four types of earthquake indicates several different mechanisms of their generation, with the role of these mechanisms varying during the seismicity increase. The first was cluster 1 at a height of ~1800 m, which was two thirds VTEs and one third SEs. The events in the horizontal clusters nos. 8 and 12 occurred at the same depth, with the percentage of VTEs decreasing in these to reach a half and below one

Table 1. Parameters of plane-oriented clusters of volcanic earthquakes occurring on Avachinsky Volcano between October 28, 2019 and December 22, 2019.

##	Date	Dip angle	Azimuth	X, m	Y, m	Z, m	K_{max}	n	S, km²	λ, %
1	29 Oct 19	1.6	110.5	489188	5900238	1842	4.2	6	2.0	67
2	31 Oct 19	66.6	262.0	489265	5900604	1512	4.9	14	1.7	79
3	4 Nov 19	81.4	72.9	489515	5900534	1647	3.5	6	0.7	50
4	4 Nov 19	57.9	288.2	489328	5900775	1292	4.5	7	0.9	57
5	6 Nov 19	82.7	242.5	489291	5900574	1407	4.5	6	0.5	100
6	6 Nov 19	81.7	69.3	489262	5900434	811	5.5	7	2.9	86
7	12 Nov 19	73.6	257.9	489179	5900771	1635	5.3	6	1.2	100
8	17 Nov 19	10.9	20.0	489197	5901039	1814	3.9	14	2.9	50
9	18 Nov 19	83.9	104.9	488982	5900870	774	3.6	10	2.7	67
10	8 Dec 19	65.6	246.1	489146	5900960	997	3.2	8	2.1	50
11	9 Dec 19	81.6	251.8	489154	5900904	302	6.6	6	2.0	80
12	10 Dec 19	6.0	221.8	489353	5900585	1813	4.4	11	0.6	27
13	21 Dec 19	71.9	239.3	488828	5901139	1332	3.9	7	2.6	29
14	22 Dec 19	59.4	348.1	489092	5900708	503	2.9	6	5.2	17
15	22 Dec 19	59.9	203.5	489338	5900679	1039	3.1	6	3.8	0

X, Y, Z are the coordinates of cluster centers (the UTM WGC-84 coordinate system); K_{max} is the highest energy class in a cluster; *n, S* are the number of earthquakes in a cluster and the cluster area; λ is the percentage of VTEs in a cluster. Subhorizontal clusters have been identified.

third, respectively. It seems that the events in these clusters mark the boundary of a subhorizontal hot magma body and reflect its response to the contact with cold meteoric water, which gives rise to explosive boiling producing fissures and VEs. It may be supposed that the body is a sill emplaced during the 1991 eruption, and the sill was thick enough to retain some plasticity. The latter circumstance produced the LPEs in cluster 12.

The subvertical clusters nos. 5 and 7 dip at similar angles (~80°−75°) and have similar dip azimuths (ENE); the events were VTEs only, which may indicate a subvertical magma body that is also in contact with meteoric water. This body may be a dike, a former conduit that supplied magma for the 1991 eruption. It is interesting to note that cluster 6, which is almost entirely composed of VTEs, has a strike azimuth that is identical both in clusters 5 and 7 (NNW−SSE), as well as a similar dip angle, but the dip azimuth is the opposite. This provides evidence that cluster 6 reflects a similar process from the opposite wall of the partially crystallized volcanic conduit. Similar azimuths occur in 8 of the 12 subvertical clusters, as well as in the fissure in the crater due to the 1991 eruption.

While the first half of the seismicity increase was dominated by VTEs with a significant amount of SEs, the role of volcano-tectonic earthquakes was afterwards gradually decreasing, special earthquakes were as good as nonexistent, and LPEs became the dominant events. This may provide evidence that brittle failure gave way to a process due to explosive boiling of aqueous fluids within the pyroclastic lava mass of the cone. The presence of long-period, special, and hybrid earthquakes shows that the mechanisms responsible for their generation are different, and that the mechanisms are combined with brittle fracture. The seismicity increase terminated in a high frequency spasmatic tremor due to intense boiling of meteoric water producing VT on December 25 and 26.

There was one unusual phenomenon in the 2019 seismicity increase, viz., luminescence in the crater and flashes above it on December 8. While the weak luminescence in the crater can be explained simply by the heating of the crater fissure due to increased flows of high temperature fumarolic gases caused by cracking in the cooling magma bodies in the volcanic cone, the bright, sudden, short-lived flashes were evidently of a different origin. The semispherical shape of the largest flash indicates that it was most likely produced by an explosion directly on the surface of the lava plug in the crater. The aspect of the light spot suggests that the flash may have been due to an explosion due to ignition of reduced volcanic gas components as they were oxidized by air oxygen. The components in question, which can make an explosive mixture when combined with air oxygen, can be primarily H_2 and CO. Since water and carbon dioxide are the main components of volcanic gases, while fluids at depth typically have an extremely low oxygen potential, their percentage may be significant.

It should be noted that explosions in air at heights of 50−200 m above the crater were recorded during the
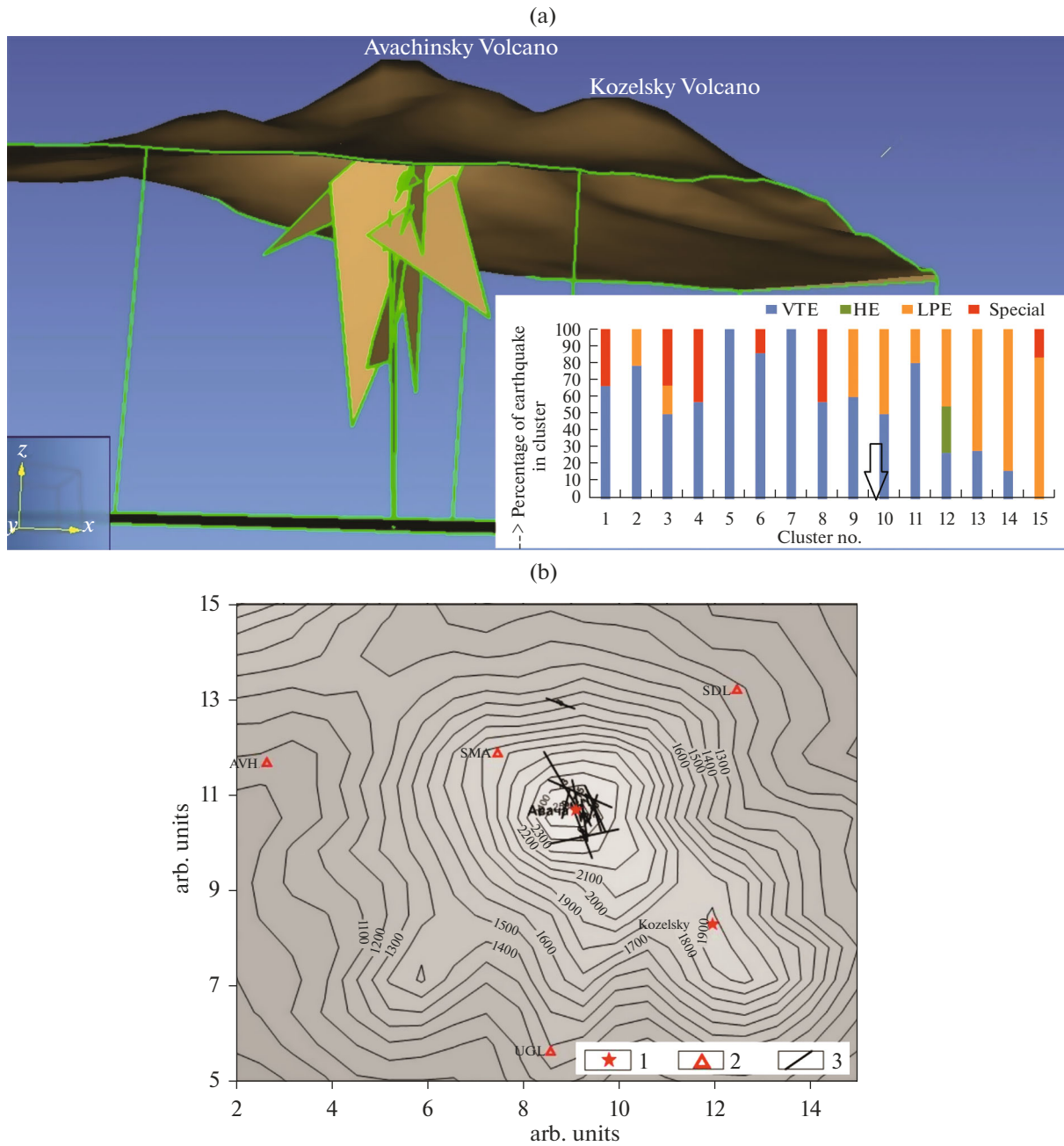
Fig. 8. A 3D visualization of VE plane-oriented clusters during October−December 2019 with the top plane at 1200 m height (a). Inset: percentage of VEs in clusters; the arrow marks explosions in air. Projections of plane-oriented earthquake clusters onto the horizontal plane at a height of 1500 m (b): (1) volcanoes; (2) RTSS; (3) projections of cluster planes.

Great Tolbachik Fissure Eruption in 1975 (Kovalev et al., 1979). As well, the shape of shock waves in air occurring during that eruption was the basis for identifying a type that originated from explosions in air due to detonation of explosion-prone gases in the atmosphere (Firstov et al., 1978). The presence of hydrogen in volcanic gases is a well-known fact, it was observed to burn at the fumarole vents on Gorelyi Volcano (Chaplygin et al., 2015; Ovsyannikov and Chirkov, 2010).

A rough estimate of fugacity for the oxygen available in the lavas discharged by the 1991 eruption of Avachinsky was obtained using an equation in (Kress and Carmichael, 1991) based on bulk rock composition from (Ivanov et al., 1995) and the compositions of small blocks ejected in 2001 (A.P. Maksimov's data). According to this rough estimate, $\log f_{O_2}$ is found within the limits from the value relevant to the equilibrium of Ni−NO to that in excess of it by one unit

$logf_{O_2}$. in the range 700−1000°C. These values are typical of island-arc andesites. Under these conditions, the molar fraction of hydrogen would be a few tenths of a percent when in equilibrium with pure H_2O. The same level of concentration would exist for CO when in equilibrium with pure CO_2. When the originally oxidizing state of the magma was in correspondence with the QFM equilibrium (quartz-fayalite-magnetite), which is characteristic for basic magmas, then the equivalent molar amounts of H_2 and CO would be a few percent. It is little likely that these low concentrations would make an explosion-prone mixture of the gases when mixed with air oxygen.

It is known that H_2 is different from the other volatiles in having a high penetrating ability at high temperatures. When its concentration has a gradient, it intensively migrates into a region of low concentration. This property is used in petrological experiments at high pressures: maintaining a hydrogen pressure from the outside, one varies its chemical potential inside sealed metal ampoules. A similar behavior is also shown by hydrogen in melts, thus affecting the oxidation state of the magmas (Gaillard et al., 2003).

The following scheme can be proposed to explain the flashes. The pressure (hence the chemical potential) of H_2 in the atmosphere is practically zero. A the same time, magmas invariably contain some amount of water, which means the presence of considerable amounts of H_2, because oxygen has low fugacity. The partial pressure of H_2 would be proportional to the total pressure and to its activity in the melt and/or a gas phase. When in the conduit of a volcano, hydrogen can experience diffusion from the residual melt to the ground surface due to the potential difference for H_2 in the atmosphere and in the magma. When sufficiently high temperatures are maintained in the conduit of the volcano, the process can also occur in the glass of the rock that was formed of the 1991 magma. Higher levels of the conduit in its colder segments may contain closed cracks (small cavities) that act as "traps" for a weak flow of H_2. The occurrence of several sudden short-lived flashes can be explained by opening of "traps" due to the ongoing seismicity increase and by the explosive response of hydrogen when mixed with air oxygen.

CONCLUSIONS

The network of RTSSs operated by the NSC GS RAS on Avachinsky Volcano enabled us to do a detailed analysis of the low magnitude seismicity observed from October to December 2019. The VE waveforms and spectral content were examined to identify three commonly accepted types, viz., volcano-tectonic, hybrid, and long period events. In addition, we identified a fourth type, a "special" type of VEs having waveforms of its own. The initial segment of SE records was dominated by lower frequencies compared with coda waves. The characteristics of these earthquakes provide indirect evidence of their being a relationship between these and the "explosive" processes occurring in the cone of the volcano.

Fifteen plane-oriented clusters have been identified in the 2019 seismicity increase of the Molodoi Konus of Avachinsky Volcano, and characteristics of the seismogenic planes have been determined. An analysis of their parameters suggests a relationship between the seismicity increase and the interaction of the hot magma bodies due to the 1991 eruption with meteoric water. The most likely cause of light flashes above the crater which were observed on December 8 seems to have been interaction of hydrogen-charged volcanic gas as it came in contact with air oxygen.

To sum up, the seismicity increase of the volcano in late 2019 was not caused by magmatic activity in the volcanic chamber. Later on, one can expect periodic repetitions of seismicity increase by interaction between the magma body that is cooling in the volcanic conduit and meteoric water. However, when seismicity appears at depths of the magma chamber (more than 2 km from the ground surface), there must be a high probability of a possible manifestation of volcanic activity.

It should be noted that Avachinsky Volcano stands 27 km from the Krai center of Kamchatka Krai and poses potential hazard to the towns of Petropavlovsk-Kamchatsky and Elizovo, and the Elizovo International Airport. In this connection, though the study of Avachinsky Volcano has been conducted during many years at the Institute of Volcanology and Seismology, RAS and by the NSC GS RAS, but short-term prediction of volcanic eruptions to high efficiency requires the monitoring of geophysical parameters near the volcano's edifice. In particular, the monitoring of the processes occurring in the upper part of the volcanic cone can be carried out using muon tomography similarly to how it is done for volcanoes of Japan and Italy (Buontempo et al., 2010; László Oláh et al., 2018).

REFERENCES

Buontempo, S., De Lellis, G., and D'Auria, L., Perspectives for the radiography of Mt. Vesuvius by cosmic ray muons, *Earth Planets Space,* 2010, vol. 62, pp. 131−137.
https://doi.org/10.5047/eps.2009.05.005

Bushenkova, N., Koulakov, I., Senyukov, S., et al., Tomographic images of magma chambers beneath the Avacha and Koryaksky volcanoes in Kamchatka, *J. Geographical Research: Solid Earth,* 2019, Iss. 9, vol. 124, pp. 9694−9713.
https://doi.org/10.1029/2019JB017952

Cannata, A., Diliberto, I.S., Alparone, S., et al., Multiparametric approach in investigating volcano-hydrothermal systems: The case study of Vulcano (Aeolian Islands, Italy), *Pure Appl. Geophys.,* 2012, vol. 169, pp. 167−182.
https://doi.org/10.1007/s00024-011-0297-z

Chaplygin, I.V., Taran, Yu.A., Dubinina, E.O., et al., The chemical composition and metal-content of magmatic gases discharged by Gorelyi Volcano, Kamchatka, *Dokl. Akad. Nauk,* 2015, vol. 463, no. 1, pp. 85.

Droznin, D.V. and Droznina, S.Ya., The DIMAS interactive program for seismic signal processing, *Seismicheskie Pribory,* 2010, vol. 46, no. 3, pp. 22−34.

Droznin, D.V. and Droznina, S.Ya., Interactive DIMAS program for processing seismic signals, *Seismic Instruments,* 2011, vol. 47, no. 3, pp. 215−224.
https://doi.org/10.3103/S0747923911030054

Dubrovskaya, I.K., Cherkashin, R.I., and Chirkov, S.A., The thermal (ThermaCam SC 640) and seismic regime of Avachinsky Volcano in 2000−2018, in *Materialy konferentsii, posvyashchennoi Dnyu vulkanologa "Sovremennyi vulkanizm i svyazannye s nim protsessy"* (Proc. conf. devoted to Volcanologist's Day "Present-Day Volcanism and Associated Processes"), March 28−29, 2019, Petropavlovsk-Kamchatsky: IViS DVO RAN, 2019, pp. 19−21.

Firstov, P.P., Adushkin, V.V., and Storcheus, A.V., Shock air waves recorded in September 1975 during the Great Tolbachik Fissure Eruption, *Dokl. Akad. Nauk SSSR,* 1978, vol. 259, no. 5, pp. 1078−1081.

Gaillard, F., Schmidt, B., Mackwell, S., and McCammon, C., Rate of hydrogen−iron redox exchange in silicate melts and glasses, *Geochim. Cosmochim. Acta,* 2003, vol. 67, no. 13, pp. 2427−2441.

Gomez, D.M., Torres, R.A., Seidl, D., et al., Tornillo seismic events at Galeras volcano, Colombia: A summary and new information from broadband three-component measurements, *Ann. Geofis.,* 1999, vol. 42, pp. 365−378.

Gordeev, E.I. and Senyukov, S.L., The 1994 seismicity increase on Koryaksky Volcano: Hybrid seismic events and their applications to seismic hazard assessment, *Vulkanol. Seismol.,* 1998, nos. 4/5, pp. 112−126.

Gorshkov, G.S., Seismic observations in 1949, *Byul. Vulkanol. St.,* 1954a, no. 21, pp. 19−39.

Gorshkov, G.S., The volcanic tremor associated with the eruption at the Bylinkina vent, *Byul. Vulkanol. St.,* 1954b, no. 23, pp. 24−33.

Gushchenko, I.I., *Izverzheniya vulkanov Mira. Katalog* (Eruptions of World Volcanoes: A Catalog), Moscow: Nauka, 1979.

Ivanov, B.V., Flerov, G.B., Masurenkov, Yu.P., et al., The dynamics and composition of the ejecta from Avachinsky Volcano in 1991, *Vulkanol. Seismol.,* 1995, nos. 4/5, pp. 5−27.

Kiryukhin, A.V., Fedotov, S.A., and Kiryukhin, P.A., A geomechanical interpretation of the local seismicity related to eruptions and renewed activity on Tolbachik, Koryakskii, and Avacha Volcanoes, Kamchatka, in 2008−2012, *J. Volcanol. Seismol.,* 2016, vol. 10, no. 5, pp. 275−291.

Kiryukhin, A.V., Fedotov, S.A., Kiryukhin, P.A., and Chernykh, E.V., Magmatic plumbing systems of the Koryakskii−Avacha Volcanic Cluster as inferred from observations of local seismicity and from the regime of adjacent thermal springs, *J. Volcanol. Seismol.,* 2017a, vol. 11, no. 5, pp. 321−334.

Kiryukhin, A., Lavrushin, V., Kiryukhin, P., et al., Geofluid systems of Koryaksky-Avachinsky Volcanoes (Kamchatka, Russia), *Geofluids,* 2017b, *Article ID* 4279652, pp. 1−21.
https://doi.org/10.1155/2017/4279652

Kovalev, G.N., Samoilenko, B.I., and Slezin, Yu.B., Volcanic explosions of air, *Dokl. Akad. Nauk SSSR,* 1979, vol. 248, no. 1, pp. 310−314.

Kress, V.C. and Carmichael, S.E., The compressibility of silicate liquids containing Fe_2O_3 and the effect of composition, temperature, oxygen fugacity and pressure on their redox states, *Contrib. Mineral. Petrol.,* 1991, vol. 108, pp. 82−92.

László Oláh, Hiroyuki K.M. Tanaka, Takao Ohminato, and Dezső Varga, High-definition and low-noise muography of the Sakurajima volcano with gaseous tracking detectors, *Scientific Reports,* 2018, issue 8: no. 3207, pp. 1−13.
https://doi.org/10.1038/s41598-018-21423-9

Malik, N.A., Zelensky, M.E., and Okrugin, V.M., The temperature and composition of fumarolic gases on Avachinsky Volcano, Kamchatka in 2013−2016, *Vestnik KRAUNTs, Nauki o Zemle,* 2017, no. 1, issue 33, pp. 21−33.

Malik, N.A. and Nekrasova, M.Yu., Multidisciplinary studies of the activity of Avachinsky Volcano in 2013 to early 2020: Ground-based, video, and seismic observations, *Vestnik KRAUNTs, Nauki o Zemle,* 2020, no. 2, issue 46, pp. 41−56.

McNutt, S.R., Seismic monitoring and eruption forecasting of volcanoes: A review of the state-of-the-art and case histories, in *Monitoring and Mitigation of Volcano Hazards,* Scarpa, R. and Tilling, R., Eds., Berlin, N. Y.: Springer-Verlag, 1996, pp. 99−146.
https://doi.org/10.1007/978-3-642-80087-0

Melekestsev, I.V., Braitseva, O.A., Dvigalo, V.N., et al., Historical eruptions of Avacha Volcano, Kamchatka: An attempt at a modern interpretation and classification for long-term prediction of the type and parameters of future eruptions. Part II (1926−1991), *Vulkanol. Seismol.,* 1994, no. 2, pp. 3−23.

Melekestsev, I.V., Seliverstov, N.I., and Senyukov, S.L., A report on resumption of activity of Avachinsky Volcano, Kamchatka in October 2001 and on studies thereof, *Vulkanol. Seismol.,* 2002, no. 2, pp. 79−80.

Milluzzo, V., Cannata, A., Alparone, S., et al., Tornillos at Vulcano: Clues to the dynamics of the hydrothermal system, *J. Volcanol. Geotherm. Res.,* 2010, vol. 198, pp. 377−393.
https://doi.org/10.1016/j.jvolgeores.2010.09.022

Minakami, T., Fundamental research for predicting volcanic eruption. Part 1, *Bull. Earthq. Res. Inst.,* 1961, vol. 38, pp. 497−544.

Moroz, Yu.F. and Gontovaya, L.I., The deep structure of the Avachinsky−Koryaksky volcanic group, Kamchatka, *Vulkanol. Seismol.,* 2003, no. 4, pp. 3−10.

Muraviev, Ya.D., On the prediction of eruptions for Avachinsky Volcano, Kamchatka, in *Materialy konferentsii, posvyashchennoi Dnyu vulkanologa "Sovremennyi vulkanizm i svyazannye s nim protsessy"* (Proc. conf. devoted to Volcanologist's Day "Present-Day Volcanism and Associated Processes"), March 29−30, 2020, Petropavlovsk-Kamchatsky: IViS DVO RAN, 2020, pp. 50−58.

Nuzhdina, I.N., Kozhevnikova, T.Yu., Toloknova, S.L., et al., The Avachinsky volcanic group, in *Zemletryaseniya Rossii v 2017 g.* (Earthquakes in Russia in the Year 2017), Obninsk: FITs EGS RAN, 2019, pp. 177.

Ovsyannikov, A.A. and Chirkov, S.A., The state of Gorelyi Volcano in June 2010, *Vestnik KRAUNTs, Nauki o Zemle,* 2010, no. 1, issue 15, pp. 10.

Power, J.A., Lahr, J.C., Page, R.A., et al., Seismic evolution of the 1989−1990 eruption sequence of Redoubt Volcano, Alaska, *J. of Volcanol. and Geotherm. Res.,* 1994, Iss. 1−4, vol. 62, pp. 69−94.
https://doi.org/10.1016/0377-0273(94)90029-9

Romashev, A.N., *Osobennosti deistviya krupnykh podzemnykh vzryvov* (The Impact of Major Underground Explosions), Moscow: Nedra, 1980.

Senyukov, S.L., Monitoring the activity of Kamchatkan volcanoes using remore observation techniques, 2000−2004, *Vulkanol. Seismol.,* 2006, no. 3, pp. 68−78.

Senyukov, S.L., Nuzhdina, I.N., Droznina, S.Ya., et al., The 1994−2005 seismicity of Avachinsky Volcano, in *Materialy nauchno-tekhnicheskoi konferentsii "Geofizicheskii monitoring Kamchatki"* (Proc. Science Conf. "Geophysical Monitoring of Kamchatka"), Petropavlovsk-Kamchatsky, January 17−18, 2006, Petropavlovsk-Kamchatsky: GS RAN, 2006, pp. 101−105.

Shakirova, A.A., Chernykh, E.V., Firstov, P.P., and Kiryukhin, A.V., A weak seismic activation of Avachinsky Volcano in October−December 2019, in in *Materialy konferentsii, posvyashchennoi Dnyu vulkanologa "Sovremennyi vulkanizm i svyazannye s nim protsessy"* (Proc. conf. devoted to Volcanologist's Day "Present-Day Volcanism and Associated Processes"), March 29−30, 2020, Petropavlovsk-Kamchatsky: IViS DVO RAN, 2020, pp. 50−58.

Tokarev, P.I., *Izverzheniya i seismicheskii rezhim vulkanov Klyuchevskoi gruppy* (1949−1963) (Eruptions and Seismicity in the Klyuchevskoi Volcanic Group: 1949−1963), Moscow; Nauka, 1966.

Uchida, N. and Sakai, T., Analysis of peculiar volcanic earthquakes at Satsuma-Iojima volcano, *Earth Planets Space,* 2002, vol. 54, pp. 197−209.

Zobin, V.M., *Introduction to Volcanic Seismology,* Third edition, Amsterdam: Elsevier, 2017.

Translated by A. Petrosyan